ISBN: 978-3-95450-240-0 ISSN: 2673-5547 doi:10.18429/JACoW-HIAT2022-TUP07

EFFICIENT HEAVY ION ACCELERATION WITH HIGH BRILLIANCE

Chuan Zhang#, GSI Helmholtz Centre for Heavy Ion Research, Darmstadt, Germany
Holger Podlech, Institute for Applied Physics, Goethe-University, Frankfurt a.M., Germany

Abstract

It is challenging to realize an efficient and brilliant RFQ for accelerating high current heavy ion beams, as space charge effects are most pronounced at the low energy end. Here "efficient" means an as short as possible accelerating structure with minimum RF power consumption, while "brilliant" means high beam transmission and low emittance growth. Using the > 9 m long HSI RFQ accelerator, one of the longest RFQs in the world, as an example, a promising solution has been presented.

INTRODUCTION

As the starting accelerating structure of the UNILAC that is the main injector to the GSI accelerator complex, the 36.136 MHz HSI RFQ can accelerate a wide variety of particle species from protons to uranium ions in the energy range of 2.2 keV/u – 120 keV/u. Some major milestones in the development of the HSI RFQ are as follows:

- In 1996: the design of the first HSI RFQ (design ion: U^{4+}, design beam current I_{in}: 16.5 emA) was started [1].
- In 1998: the first HSI RFQ (hereafter referred to as Version-1998) was constructed [2].
- In 1999: the Version-1998 RFQ was put into operation.
- In 2004: the electrodes were renewed with an improved radial matching section for a larger acceptance.
- In 2008: the second HSI RFQ (hereafter referred to as Version-2008) was designed (still for U^{4+} but I_{in} was increased to 20 emA) and produced [3]. For this upgrade, the inter-vane voltage U was increased from 125 kV to 155 kV.
- In 2009: the Version-2008 RFQ was put into operation.
- From 2009 until now: the Version-2008 RFQ is in routine operation (in 2019, the electrodes were renewed but still based on the same design).
- Since 2015: in order to meet the beam intensity requirement for FAIR, the R&D for a third version of the HSI RFQ has been started.

The main design parameters of the two constructed HSI RFQs can be found in Table 1. The design goals for the new version are as follows:

- I_{in} = 20 emA with $T \geq 90\%$ (for real operation, 18 emA and 16.2 emA will be expected at the entrance and the exit of the RFQ, respectively).
- The maximum surface electric field $E_{s,\,max}$ should be lower than that of the Version-2008 RFQ.
- L should be kept same so that the same tank can be used.

email address: c.zhang@gsi.de

Table 1: Design Parameters of the Constructed HSI RFQs

Parameters	Version-1998	Version-2008
W [keV/u]	2.2 – 120	2.2 – 120
U [kV]	125	155
I_{in} [emA]	16.5	20
$\varepsilon_{t,\,in,\,un,\,total}$ [π mm-mrad]	138	210
$\varepsilon_{t,\,in,\,n,\,rms}$ [π mm-mrad]	0.050	0.076
$\alpha_{Twiss,\,t,\,in}$	0.43	0.6
$\beta_{Twiss,\,t,\,in}$ [cm/rad]	4.6	13.6
$E_{s,\,max}$ [MV/m]	31.8	31.2
L [cm]	921.749	921.7
T [%]	89.5	88.5

DESIGN STRATEGY

For the third HSI RFQ, several solutions have been already proposed:

- In 2016: using one single cavity with U = 125 kV [4] and $E_{s,\,max}$ = 30.2 MV/m.
- In 2020: using multiple short and independent cavities with $E_{s,\,max}$ = 30.9 MV/m (U varies from 120 kV to 147 kV, but it is constant in each cavity) [5].

All these solutions have not only lowered maximum surface electric field of the electrodes but also improved beam performance.

The motivation for this new study is to develop another single-cavity design at U = 120 kV to further lower $E_{s,\,max}$, save more RF power, and improve beam quality.

The brilliance is an important index to measure the beam quality. There are different definitions for the brilliance B and the one used by this study is given as follows:

$$B \equiv \frac{I}{\varepsilon_x \varepsilon_y}. \quad (1)$$

where I is the beam current in mA and ε_x and ε_y are the transverse emittances in π mm mrad (for B, the factor $1/\pi^2$ can be left out). No matter which definition is used, for a given input beam, a design with a high B means high beam transmission and low emittance growth.

For the new HSI RFQ design with U = 120 kV (hereafter referred to as Design-2022), the high efficiency has been achieved by using the New Four Section Procedure that

Content from this work may be used under the terms of the CC BY 4.0 licence (© 2022). Any distribution of this work must maintain attribution to the author(s), title of the work, publisher, and DOI

ISBN: 978-3-95450-240-0 ISSN: 2673-5547 doi:10.18429/JACoW-HIAT2022-TUP07

Content from this work may be used under the terms of the CC BY 4.0 licence (© 2022). Any distribution of this work must maintain attribution to the author(s), title of the work, publisher, and DOI

supports to realize a fast main bunching with a relatively low U under balanced transverse and longitudinal forces [6], and the high brilliance has been achieved by using the recently developed MEGLET (Minimizing Emittance Growth via Low Emittance Transfer) method [7]. Different from previously proposed methods, which always try to avoid emittance transfer, the MEGLET method minimizes emittance growth by:

- Allowing low emittance transfer when the ratio of transverse emittance to longitudinal emittance can be held in the range of $0.9 \leq \frac{\varepsilon_l}{\varepsilon_t} \leq 1.4$ (see Fig. 1).
- Using two emittance-transfer periods (in which the emittance transfer is in opposite directions) to minimize the net emittance growth.

To obtain a high B for the new HSI RFQ, the emittance transfer in the 2nd period has been designed to be stronger than that in the 1st period so that one can get smaller transverse output emittances.

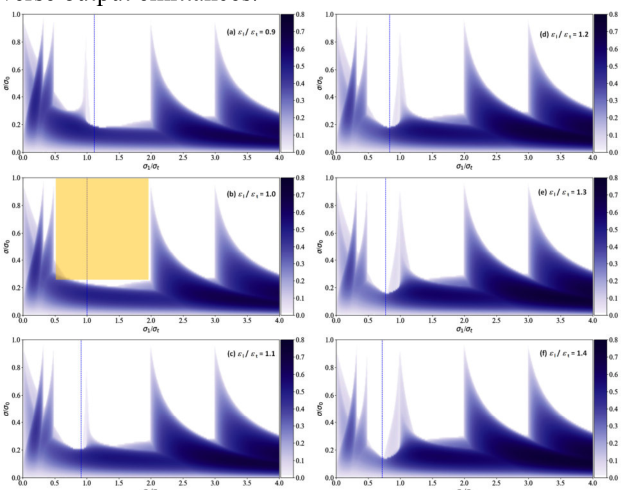

Figure 1: Hofmann charts (generated using TraceWin [8]) for the emittance ratios $\frac{\varepsilon_l}{\varepsilon_t} = 0.9 - 1.4$ [7]. The rectangle marked in orange covers the safe area for tune footprints.

DESIGN-2022 HSI RFQ

Figure 2 shows the evolution of the main parameters along the Design-2022 HSI RFQ.

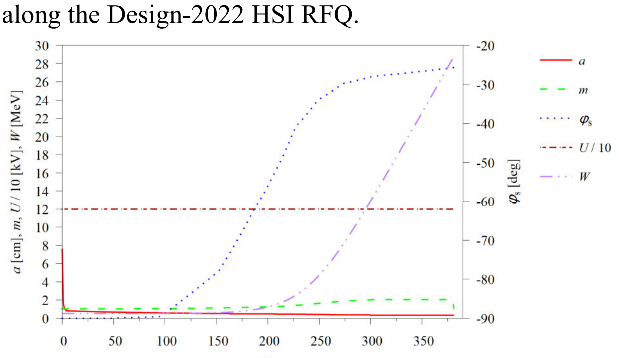

Figure 2: Main design parameters of the Design-2022 HSI RFQ, where a is the minimum electrode aperture, m is the electrode modulation, φ_s is the synchronous phase, U is the inter-vane voltage, and W is the beam energy.

In Table 2, one can see that:

- U is ~ 25% lower in the new design, which will considerably save the RF power (the power is proportional to U^2).
- $E_{s,\,max}$ becomes < 30 MV/m.
- The average mid-cell aperture of the electrodes $r_{0,\,avg.}$ is now only 0.02 cm smaller so that the current rings for carrying electrodes should be still applicable.
- The new RFQ is slightly shorter, which leaves a little room for the fine tuning of the design.

Table 2: Comparison between the Version-2008 and Design-2022 HSI RFQs

Parameters	Version-2008	Design-2022
U [kV]	155	120
$r_{0,\,avg.}$ [cm]	0.60	0.58
$E_{s,\,max}$ [MV/m]	31.2	29.9
Total number of cells	409	381
L [cm]	921.7	920.1

The beam dynamics simulation of the Design-2022 HSI RFQ was performed using the PARMTEQM (PAR) code [9] with a 4D Waterbag (particles are generated randomly in a 4D transverse hyperspace with a uniform phase spread and no energy spread) input distribution. The same input emittances ($\varepsilon_{t,\,in,\,un,\,total} = 210\ \pi$ mm mrad or $\varepsilon_{t,\,in,\,n,\,rms} = 0.076\ \pi$ mm mrad) and Twiss parameters (see Table 1) as the Version-2008 were adopted. The Design-2022 is also checked with an input distribution generated by the DYNAC (DYN) code [10] with $\varepsilon_{t,\,in,\,n,\,rms} = 0.076\ \pi$ mm mrad and the same Twiss parameters (but in the transverse directions, the distributions are Gaussian). The transverse phase spaces of the two used input distributions are shown in Fig. 3, which shows that the beam size and the maximum divergence angle are much larger in the Gaussian case.

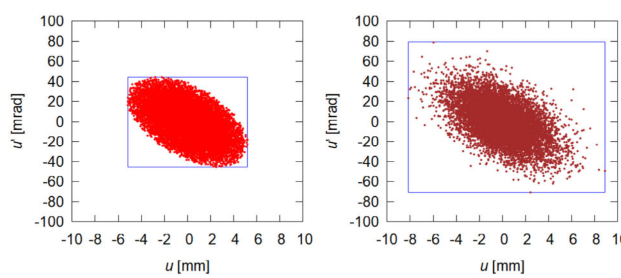

Figure 3: 4D Waterbag (left) and Gaussian (right) transverse input distributions (u represents the x or y direction).

In Fig. 4 and Fig. 5, the longitudinal and transverse emittances are plotted as functions of cell number for the Waterbag and Gaussian cases, respectively, where the emittance curves for 99% of particles are used to show the performance of the main beam by excluding 1% outmost particles. In the part marked in orange, the tune footprints of the beam are inside the so-called "safe rectangle" with $0.5 \leq \frac{\sigma_l}{\sigma_t} \leq 2.0$ and $0.25 \leq \frac{\sigma}{\sigma_0} \leq 1.0$ (corresponding to the area marked in orange in Fig. 1). Generally speaking, the two

ISBN: 978-3-95450-240-0 ISSN: 2673-5547 doi:10.18429/JACoW-HIAT2022-TUP07

figures are similar. For the Waterbag case, the emittance ratio of the main beam is well held in the range of $0.9 \leq \frac{\varepsilon_l}{\varepsilon_t} \leq 1.4$ along the main part of the RFQ, as required by the MEGLET method. For the Gaussian case, the emittance transfer is stronger, but the maximum emittance ratio of the main beam is 1.7, still not far away from the optimum range.

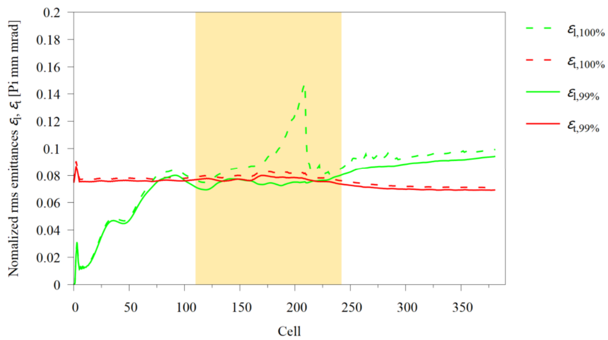

Figure 4: Evolution of emittances for 100% and 99% of particles along the Design-2022 HSI RFQ (Waterbag case).

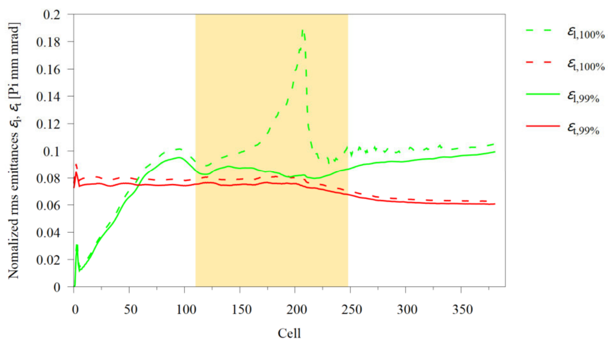

Figure 5: Evolution of emittances for 100% and 99% of particles along the Design-2022 HSI RFQ (Gaussian case).

BENCHMARK

For a benchmark, the DYNAC code [10] has been taken. A comparison of the main simulation results given by the two codes is made in Table 3, which shows that no matter beam transmission or output emittances are comparable.

Table 3: Simulated beam transmission and normalized rms output emittances (π mm mrad)

	PAR Waterbag	PAR Gaussian	DYN Waterbag	DYN Gaussian
T [%]	96.2	90.3	96.1	90.9
$\varepsilon_{x,\text{ out}}$	0.070	0.063	0.079	0.068
$\varepsilon_{y,\text{ out}}$	0.072	0.063	0.077	0.068
$\varepsilon_{z,\text{ out}}$	0.099	0.105	0.088	0.097

With the Gaussian input beam, more losses happened due to the larger total emittance (see Fig. 3). But for all cases, the beam transmission is still > 90%. Except the transverse emittances of the DYNAC simulation in the Waterbag case are slightly > $\varepsilon_{t,\text{ in, n, rms}}$, all other transverse emittance values are much smaller than $\varepsilon_{t,\text{ in, n, rms}}$. This indicates a high brilliance of the Design-2022 HSI RFQ. As 120 kV is much lower than 155 kV used by the current HSI RFQ, the efficiency of the Design-2022 HSI RFQ can be clearly seen.

Figures 6 shows that the output particle distributions simulated by DYNAC are similar to those given by PARMTEQM for both the Waterbag case and the Gaussian case, especially in the transverse planes.

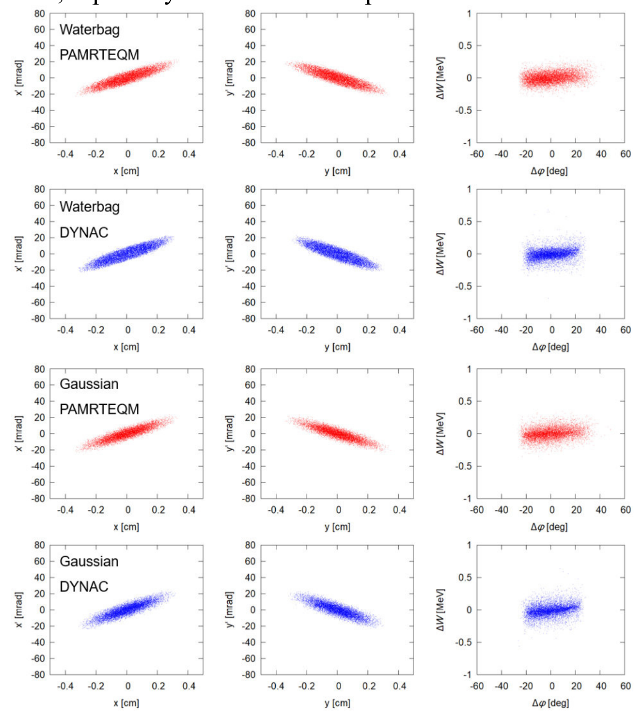

Figure 6: Output particle distributions.

ACKNOWLEDGEMENTS

Special thanks go to Hartmut Vormann for providing the information about the two constructed HSI RFQs and Eugene Tanke for the discussions on the DYNAC simulation.

REFERENCES

[1] A. Schempp, "Design of Compact RFQ's", in *Proc. 1996 Linear Accelerator Conf. (LINAC'96)*, Geneva, Switzerland, 26-30 August 1996, pp. 53-55, paper MOP03.

[2] U. Ratzinger, K. Kaspar, E. Malwitz, S. Minaev, and R. Tiede, "The GSI 36 MHz High-Current IH-Type RFQ and HIIF–Relevant Extensions", *Nuclear Instruments and Methods in Physics Research Section A: Accelerators, Spectrometers, Detectors and Associated Equipment*, vol. 415, issues 1–2, pp. 281-286, 21 September 1998, doi:10.1016/S0168-9002(98)00395-7

[3] A. Kolomiets, S. Minaev, W. Barth, L. Dahl, H. Vormann, and S. Yaramyshev, "Upgrade of the Unilac High Current Injector RFQ", in *Proc. 2008 Linear Accelerator Conf. (LINAC'08)*, Victoria, BC, Canada, 29 September – 3 October 2008, pp. 136-138.

[4] C. Zhang, L. Groening, O. Kester, S. Mickat, H. Vormann, M. Baschke, H. Podlech, U. Ratzinger, and R. Tiede, "HSI RFQ Upgrade for the UNILAC Injection to FAIR", in *Proc. 2016 IPAC'16*, Busan, Korea, May 8-13, 2016, pp. 877-879. doi:10.18429/JACoW-IPAC2016-MOPOY016

[5] C. Zhang, H. Podlech, and E. Tanke, "Realizing Long Radio-Frequency Quadrupole Accelerators with Multiple Shorter

Content from this work may be used under the terms of the CC BY 4.0 licence (© 2022). Any distribution of this work must maintain attribution to the author(s), title of the work, publisher, and DOI

ISBN: 978-3-95450-240-0 ISSN: 2673-5547 doi:10.18429/JACoW-HIAT2022-TUP07

Content from this work may be used under the terms of the CC BY 4.0 licence (© 2022). Any distribution of this work must maintain attribution to the author(s), title of the work, publisher, and DOI

[5] C. Zhang, H. Podlech, and E. Tanke, "Realizing Long Radio-Frequency Quadrupole Accelerators with Multiple Shorter and Independent Cavities", *Physical Review Accelerators and Beams*, vol. 23, no. 042003, April 2020, doi:10.1103/PhysRevAccelBeams.23.042003

[6] C. Zhang and A. Schempp, "Beam dynamics studies on a 200mA proton radio frequency quadrupole accelerator," *Nuclear Instruments and Methods in Physics Research Section A: Accelerators, Spectrometers, Detectors and Associated Equipment*, vol. 586, no. 2, pp. 153–159, Feb. 2008. doi:10.1016/j.nima.2007.12.001

[7] C. Zhang, "Minimizing Emittance Growth via Low Emittance Transfer", *Physical Review Accelerators and Beams*, vol. 25, no. 034201, March 2022, doi:10.1103/PhysRevAccelBeams.25.034201

[8] TraceWin code, http://irfu.cea.fr/dacm/logiciels/

[9] *Manual of the LANL RFQ Design Codes*, LANL Report No. LA-UR-96-1836, Jun. 2005.

[10] DYNAC, https://github.com/dynac-source/dynac-source